Short-hairpin RNA against aberrant *HBB*$^{IVSI-110(G>A)}$ mRNA restores β-globin levels in a novel cell model and acts as mono- and combination therapy for β-thalassemia in primary hematopoietic stem cells

Petros Patsali,[1,2] Panayiota Papasavva,[1,3] Coralea Stephanou,[1,2] Soteroulla Christou,[4] Maria Sitarou,[4] Michael N. Antoniou,[2] Carsten W. Lederer,[1,3,†,] and Marina Kleanthous[1,3,†]*

[1]Department of Molecular Genetics Thalassaemia, The Cyprus Institute of Neurology and Genetics, Nicosia, Cyprus; [2]Department of Medical and Molecular Genetics, King's College London, UK; [3]Cyprus School of Molecular Medicine, Nicosia, Cyprus and [4]Thalassaemia Centre, Ministry of Health, Cyprus

†Shared last authors

Correspondence: lederer@cing.ac.cy
doi:10.3324/haematol.2018.189357

Supplementary Data

Short-hairpin RNA against aberrant *HBB*$^{IVSI-110(G>A)}$ mRNA restores β-globin levels in a novel cell model and acts as mono- and combination therapy for β-thalassemia in primary hematopoietic stem cells

Petros Patsali[1,2], Panayiota Papasavva[1,3], Coralea Stephanou[1,2], Soteroulla Christou[4], Maria Sitarou[4], Michael N. Antoniou[2], Carsten W. Lederer[1,3,†,*], Marina Kleanthous[1,3,†]

[1] Department of Molecular Genetics Thalassaemia, The Cyprus Institute of Neurology and Genetics, 1683 Nicosia, Cyprus
[2] Department of Medical and Molecular Genetics, King's College London, London, SE1 9RT, United Kingdom
[3] Cyprus School of Molecular Medicine, 1683 Nicosia, Cyprus
[4] Thalassaemia Centre, Ministry of Health, Cyprus
[*] Corresponding author
[†] Shared last authors

Corresponding author

Correspondence should be addressed to C.W.L. (Lederer@cing.ac.cy), Nicosia, Cyprus

Carsten W Lederer, PhD, Molecular Genetics Thalassaemia Department, The Cyprus Institute of Neurology and Genetics, 6 International Airport Avenue, 1683 Nicosia, Cyprus. Telephone: +357-22-392764. Fax: +357-22-392615.

Running title

Therapy by shRNAs against aberrant HBB mRNA

Supplementary methods

Use of lentiviral vectors

Production in HEK293T cells and qPCR-based measurement of biological titers based on transduction of HEL cells (Supplemental Table S2) were performed as published.[1] For functional study, cells were transduce with hourly agitation for six hours before replacement of medium, as described elsewhere.[2] After initial transductions for each vector at a multiplicity of infection (MOI) of 5, 10 and 20 and after measurement of vector copy numbers per haploid genome (VCN), MOI was modified for each vector towards a VCN of 3 for GLOBE and a VCN of 20 for shRNA-encoding vectors in order to achieve saturating treatment for the latter. For combination treatments with shRNA-encoding vectors and the GLOBE gene-addition vector, cells were first transduced with the GLOBE vector and after a time interval of 24 h with the shRNA-encoding vector.

HBB (β-globin) mutagenesis

The *HBB*$^{IVSI\text{-}110(G>A)}$ mutation was introduced into a transfer plasmid encoding the GLOBE vector using the QuikChange Lightning Site-Directed Mutagenesis Kit (*Agilent Technologies, Germany*) according to the manufacturer's instructions. To this end, we used the GLOBE transfer plasmid as template and primers IVSI-110_Mut_FW and IVSI-110_Mut_RV (Supplemental Table S1) for mutagenesis by PCR. After *Dpn*I endonuclease removal of parental DNA template, the resulting mutated DNA was transformed into chemically competent XL10-Gold bacteria (*Agilent Technologies, Germany*), and correct GLOBE$^{IVSI\text{-}110(G>A)}$ clones were confirmed by sequencing (*Applied Biosystems, Foster City, CA*) (Fig 1B).

Cloning of RNA interference vectors

Short-hairpin RNAs targeting the *HBB*$^{IVSI\text{-}110(G>A)}$-specific transcript sequence were designed according to published guidelines of the RNA interference (RNAi) consortium (TRC),[3] as detailed in the main text and shown in Figure 2, and were assembled by annealing synthetic oligonucleotides (*Metabion International AG, Germany*) for cloning in the *Eco*RI and *Age*I sites of the pLKO.1 TRC lentiviral transfer vector (Addgene plasmid # 10878, a gift from David Root) for comparison with mock treatment and for treatment with the pLKO.1 Scramble vector (Addgene plasmid # 1864, a gift from David Sabatini). Positive *E. coli* (*New England Biolabs, Ipswich, MA*) clones were confirmed by restriction enzyme digestion and sequencing across both ligation sites, prior to use of plasmid preparations (*Macherey-Nagel GmbH, Germany*) in lentiviral vector production.

Culture, transgenesis and clonal selection of MEL cells

MEL cells were cultured in cRPMI supplemented with 10% FBS, 1x penicillin/streptomycin and 1% 100-mM L-glutamine, (all *Invitrogen, Thermo Fisher Scientific, UK*) in 10-cm diameter dishes (*Corning, USA*) and maintained at 250 000–500 000 cells/mL. Terminal erythroid differentiation was induced by addition of 1.5% DMSO to cultures of 100 000–200 000 cells/mL. Cells were collected for RNA and protein analysis at day 3 and day 6 – 9 post-induction, respectively. MEL cells were transduced as described,[2] using the GLOBE vector[4] to produce positive controls for normal HBB expression and the GLOBE$^{IVSI\text{-}110(G>A)}$ vector to produce cells emulating the human *HBB*$^{IVSI\text{-}110(G>A)}$ splice defect. VCN was determined for lentiviral vectors (LVs) as described,[1] and pools of cells for HBB expression (MEL-*HBB* with average VCN 2.0) and *HBB*$^{IVSI\text{-}110(G>A)}$ expression (MEL-*HBB*^{IVS} with average VCN 1.9) were selected for further experiments.

To isolate transgenic clones, MEL-*HBB*^{IVS} cells (average VCN 1.9) were diluted to working concentrations of 1.5 cells / 100 μL cRPMI and seeded into six 96-well plates. Cells were cultured for 48 h without moving the plates to achieve distinguishable growing colonies that were easy to score under the microscope. Wells with single clones were expanded to 24-well plates and VCN was assessed by qPCR as described.[1] Transduction for shRNA and combination treatments employed MEL-*HBB*^{IVS} VCN 1 to test correction and MEL-*HBB* LV as positive control.

Isolation and culture of CD34$^+$ cells

Primary human CD34$^+$ cells, representing HSPCs, were isolated from 7 to 25 mL of naïve same-day peripheral blood using Accu-Prep Lymphocytes (*Axis-Shield PoC AS, Ireland*). Procedures for handling, transduction and culture were as described,[2] with additional CD34$^+$ magnetic-activated cell sorting (*Miltenyi Biotec, Germany*)

after buffy-coat isolation and before expansion culture. Cells were expanded for up to ten days before transduction. For combination treatments with shRNA-encoding vectors and the GLOBE gene-addition vector, cells were first transduced with the GLOBE vector and after a time interval of 24 h with the shRNA-encoding vector. Monotherapy for shRNAs was applied the same day as shRNAs for combination treatment. At the earliest 48 h after the last transduction, cells were transferred to differentiation medium, made up of 70% MEM Alpha (*Corning Cellgro*, *USA*), 30% defined FBS (*Hyclone GE Healthcare*, *US*), 10 μM 2-mercapto-ethanol (*Sigma-Aldrich GmbH*, *Germany*), 10 U/mL erythropoietin (*Amgen*, *USA*), 10 ng/mL stem cell factor (*Peprotech Inc.*, *USA*), 1x penicillin-streptomycin (*Corning Cellgro US*), where they were kept at 0.5–1 x 10^6 cells/mL for up to five days before sample collection for microscopy and reversed-phase high-performance liquid chromatography (HPLC).

Immunoblotting

Lysates equivalent to 0.5–1 x 10^6 cells per well were separated by polyacrylamide gel electrophoresis and blotted onto nitrocellulose Parablot NCP membranes (*Macherey-Nagel GmbH*) using wet electrophoretic transfer. After temporary staining with Ponceau Red solution (*Sigma-Aldrich, St. Louis, MO*) to confirm quantitative protein transfer, membranes were blocked and incubated with the appropriate primary antibody, specifically Mouse-αHuman HBB (@1:1000; clone 37-8; #sc-21757), Rabbit-αMouse Hba (@1:1000; H80; #sc-21005)(all *Santa Cruz Biotechnologies, Dallas TX*) or Mouse-αMouse-Actb (@1:10000; clone AC-15; #A1978; *Sigma-Aldrich*), before washes and incubation with the corresponding horseradish-peroxidase-conjugated secondary antibody, specifically Goat-αMouse-IgG(H+L) (#115-035-003) or Goat-αRabbit-IgG(H+L) (#111-035-003) (both @1:10000; *Jackson ImmunoResearch Laboratories, UK*). Bands were visualized using chemiluminescence detection (*Lumisensor, GenScript, Piscataway, NJ*), and a Bio-Rad Imaging system and ImageLab Software 5.1 (*Bio-Rad Laboratories, Inc., Hercules, CA*) were used for image acquisition and quantification of band densities.

The correction level of HBB protein levels was measured as the fold-change of the ratio of HBB/Hba (α-globin) chain band intensities, to normalize for variable differentiation. As specified in the main text, HBB/Hba values are given either as percentage relative to the highest same-experiment sample intensity, as fold change relative to that of the mock-treated MEL-*HBB*$^{IVSI-110(G>A)}$ negative control, or as percentage relative to the mock-treated MEL-*HBB* positive control. The level of differentiation was measured as fold-change in the level of murine Hba chains compared to mock-treated control. Murine Actb was included in all immunoblots and used as same-gel, same-membrane calibrator for equal loading of samples for HBB and Hba detection.

Microscopy

Cell death was monitored by scoring unprocessed trypan-blue-stained cells in culture aliquots. Morphological characterization of HSPC-derived erythroid subpopulations at the culture end point was based on cytocentrifugation of 0.5–1 x 10^5 cells in a Cellspin II cytocentrifuge (*Tharmac, Germany*) and dianisidine staining before standard May-Grünwald-Giemsa (all *Sigma-Aldrich*) staining and preservation under mounting medium (Entellan, *Merck, Germany)*. Microscopic analyses were chosen in preference to flow cytometry for reasons of sample scarcity and of the higher level of information obtained by skilled morphological observation. Images were acquired using an IX73P1F inverted microscope, LED illumination, a 40× lens and averaging of seven frames per image in CellSens 1.7 (*Olympus Corporation, Germany*). Morphology of cells was analyzed by treatment-blinded scoring of between four and five photographs (depending on cell density) for each sample, representing between 400 and 500 cells per image. Erythroid-lineage cell types are distinguished by cell size, coloring and morphology of cell and nucleus, and by level of hemoglobinization, in line with criteria outlined in Wintrobe's Clinical Hematology[5] and facilitated by additional dianisidine staining of hemoglobin.

Reversed-phase high-performance liquid chromatography

Differentiated $CD34^+$-derived primary cells were lysed in 50 μL of HPLC-grade water per 0.5 x 10^6 cells, centrifuged at 4 °C and 21100 RCF, and 40 μL

of the supernatant injected per analysis on a Shimadzu Prominence system. In modification of previously described procedures,[6] separation with a linear gradient of acetonitrile/methanol (both *Merck*) against 0.1% trifluoroacetic acid (*Sigma-Aldrich*) utilized a Jupiter 5-µm C18 25-cm column with 4.6 mm diameter (*Phenomenex, Torrance, CA*) and acquisition of the absorbance readout at 259 nm. After treatment-blinded manual correction of automatic peak detection, the ratio of peak areas for β-like globins to HBA1/2 (HBA) was used for comparison of relative, respectively, HBB, HBG1 (^{A}g-globin), HBG2 (^{G}g-globin), HBG1/2 (HBG) and total β-like globin (HBx) quantities. This study did not quantify membrane-bound α-globin in erythrocyte ghosts and its possible reduction after treatment of thalassemic samples. Measurement by HPLC alone may therefore give an underestimation of the true correction of HBB/HBA levels achieved.

Messenger RNA quantification

RNA was extracted using Trizol and treated with DNase I (both *Invitrogen/Thermo Fisher Scientific*) before reverse transcription using the TaqMan Reverse Transcription PCR kit (*Applied Biosystems*). The equivalent of 12.5 ng/µL cDNA were measured per sample and triplicate non-template controls included in each PCR run on a 7900HT Fast Real-Time PCR System (*Applied Biosystems*). Variant-specific quantification of samples was performed by duplex PCR with the Multiplex PCR Kit (*Qiagen, Germany*), in triplicate against a plasmid-based standard curve holding the aberrant and normal amplicons. Quantities of total *HBB*$^{IVSI-110(G>A)}$-derived RNAs were determined by the ΔΔCT method and SYBR Green-based RT-qPCR detection of all *HBB* transcripts with exon-1-specific primers, against *Hba* as calibrator. Variant-specific contribution to total detected quantities were calculated based on probe-based calculation of variant ratios. For sequences of primers and probes (*Metabion International AG*), see Supplementary Table S1.

Statistical analyses

After data handling in Excel (Office 2010, *Microsoft Corp., Cyprus*), statistical analyses were performed in Prism 7.0 (*GraphPad Software Inc., La Jolla, CA*). The Shapiro-Wilk normality test was used to determine sample distribution and the appropriate test for group comparisons. One-way ANOVA with Dunnett's or Tukey's multiple comparison test, as appropriate, was used to compare normally distributed data, for others the non-parametric Kruskal-Wallis test with Dunn's multiple comparison test; all tests are non-directional. Summary statistics are given as geometric mean ± geometric standard deviation for fold-changes and normalized data centered around 1, and as arithmetic mean ± standard deviation of the population mean for other data. The number of replicates given are biological replicates throughout. Asterisks in graphs indicate the level of significance in line with convention, for *P* values below 0.05 (*), 0.01 (**), 0.001 (***) or 0.0001 (****), respectively.

Supplementary discussion

Based upon the hypothesis that aberrant mRNA interferes with normal HBB expression we targetted aberrant *HBB*$^{IVSI-110(G>A)}$ mRNA by shRNAs as a means of improving *HBB*$^{IVSI-110(G>A)}$ disease pathology. Four different shRNAs (*Up*, *Mid*, *Mid2* and *Down*) targeting three overlapping sequences specific for aberrant *HBB*$^{IVSI-110(G>A)}$ mRNA were expressed from RNApolIII-driven LVs, with *Mid2* harboring a modified passenger strand compared with *Mid* to avoid premature termination of transcription.

Initial analyses were performed in two transgenic erythroid cell lines, MEL-*HBB*$^{IVSI-110(G>A)}$ and MEL-*HBB*, which faithfully represented known features of *HBB*$^{IVSI-110(G>A)}$-thalassemia. Functional assessment of *HBB*$^{IVSI-110(G>A)}$-specific shRNAs in the MEL model showed significant increase of normal to aberrant *HBB* mRNA ratios for *Down*, without significant ratio or quantity differences for the other shRNAs. Remarkably, corresponding immunoblots showed significant 9.1- and 10.8-fold induction of HBB protein levels by *Mid* and *Mid2*, respectively, and merely 2.8-fold induction by *Down* without statistical significance. At both mRNA and protein level, *Mid* and *Mid2* gave similar results, despite the latter's potential advantage in RNApolIII-driven expression. This might come about by inefficient action of the dT_4 sequence as terminator and is complicated in its interpretation by the possibility that differences in the stem structures for *Mid* and *Mid2* shRNA may also

differentially affect interaction with AGO2 and thus RNAi activity.[9] Importantly, therapeutic application of our shRNA-based strategy would rely on regulated, RNApolII-driven shRNA expression, for which the dT_4 sequence harbored by the *Mid* shRNA would be of no consequence.

Application of our shRNAs in $CD34^+$ cells from *HBB*$^{IVSI-110(G>A)}$-homozygous patients resulted in significant correction of lineage differentiation for *Mid* and *Mid2*, in accordance with protein results in MEL-*HBB*$^{IVSI-110(G>A)}$. Additionally, application of *Mid* or *Mid2* on their own or of *Mid* in combination with *GLOBE* surpassed correction of erythroid differentiation by *GLOBE* alone. Likewise, only *GLOBE+Mid* gave significant improvement in the number of hemoglobinized cells. These microscopy findings were mirrored by relative HBB abundance, with significant correction by *Mid* and *Mid2* and significant improvement of *GLOBE+Mid* compared with *GLOBE* alone.

GLOBE had only minor incremental effect in combination treatment. One reason for this observation may be the superiority of full-length endogenous control elements of both *HBB*$^{IVSI-110(G>A)}$ alleles compared to the reduced elements held by the GLOBE vector. Another may be the β^+ status of *HBB*$^{IVSI-110(G>A)}$ thalassemia, which generally decreases the sensitivity of hemoglobinization and HBB/HBA ratios as assessment criteria.[8] This was aggravated by high baseline HBB/HBA ratios for *HBB*$^{IVSI-110(G>A)}$-homozygous cells in our liquid cultures (0.41), which exceeded those for peripheral blood even of patients with (milder) thalassemia intermedia (0.23).[7] The latter point may not only further conceal contributions by GLOBE in combination therapy, but also likely resulted in a general underestimation of effects for any of our vectors in liquid cultures, compared to what may be observed in patients.

As one explanation for the discrepancy between mRNA and protein data in MEL-*HBB*^{IVS} cells, *Mid* and *Mid2* shRNAs might translationally block rather than degrade aberrant *HBB* mRNA. Conversely, *Down* shRNA, which appears to knock down aberrant RNA, also has six nucleotides perfect complementarity and additional stabilizing interactions with normal *HBB* mRNA and might thus translationally block normal *HBB* production. For all three shRNAs, this would tie in with the observed mRNA and protein levels in transgenic MEL cells and with the latest insights into co-translational regulation of gene expression. In a recent seminal paper, Yordanova et al. established ribosome stalling, queueing and steric inhibition of further translation as a co-translational regulatory mechanism for transcripts with multiple in-frame stop codons.[10] This observation suggests a ready means of ribosome sequestration by aberrant *HBB*$^{IVSI-110(G>A)}$ transcripts and gives credence to an original tentative model of co-translational interference in HBB$^{IVSI-110(G>A)}$ thalassemia proposed by Breda *et al.*[11] It would moreover predict an alleviation of ribosome sequestration by a *Mid*- or *Mid2*-mediated translation block upstream of the aberrant HBB$^{IVSI-110(G>A)}$ stop codon, and in combination therapy would be of equal importance for gene therapy by gene addition and by activation of endogenous γ-globin. Importantly, the data in hand for *GLOBE+Mid* combination treatment cannot discern potentially differential effects of shRNAs on globin production from *HBB*$^{IVSI-110(G>A)}$ and from normal loci. This point could be addressed using shRNA combination treatment with induction of endogenous γ-globin[12] or with distinct exogenous β-like globins, such as our *GLOBE*-derived MA821^{T87Q} vector.[1]

Owing to both nuclear and cytosolic shRNA action[13,14] and based on various complementarities at the DNA, pre-mRNA and mRNA level, our shRNAs may act by yet further mechanisms. For instance, similar to interference of antisense RNAs with splice-site recognition, the antisense strands of any of the four *HBB*$^{IVSI-110(G>A)}$-specific shRNAs may variously block aberrant and normal splice consensus sites or their associated sequence context. Our preliminary RNA data in MEL-HBB^{IVS} indicate that the sum of these effects would not greatly shift the balance between aberrant or normal transcripts but may interfere with overall *HBB*$^{IVSI-110(G>A)}$-derived mRNA abundance, which could be tested by application of corresponding antisense oligonucleotides. Their action would differ from that of a 14-nucleotide antisense morpholino sequence reported elsewhere,[15] which achieved *HBB*$^{IVSI-110(G>A)}$ splice correction by pre-mRNA-specific binding of the aberrant splice acceptor, at only seven contiguous nucleotides

complementarity with aberrant RNA. Indeed, in cases of stable transcripts with aberrant exon boundaries, splice correction by non-permanent delivery of antisense oligonucleotides would normally be suggested.[16,17] However, the present study indicates that action by LV-encoded shRNAs and a resulting increase of normal protein production from the mutant locus should be investigated as a potentially superior therapeutic option. Our findings in MEL-*HBB*$^{IVSI-110(G>A)}$ and CD34^{+} cells are therefore not only important for our understanding of disease causation and therapy development for *HBB*$^{IVSI-110(G>A)}$ β-thalassemia, but also as an analysis and therapy approach for other diseases.

Clinical translation of the present approach requires shRNA expression at defined VCN and from stage- and lineage-specific promoters. Low VCNs minimize risk of insertional mutagenesis and other side effects of high-level shRNA delivery,[18] such as might have been the delayed differentiation of MEL-*HBB*$^{IVSI-110(G>A)}$ cells and the increased cell death in primary cultures observed here. To this end, expression of intronic shRNAs under RNApolII promoters can be predicted to avoid the interferon response,[19] but our initial attempts to replicate the corresponding design proposed by Samakoglu *et al.*[20] did not lead to detectable target knockdown (data not shown). Importantly, Brendel *et al.*[21] successfully employed control elements of the *GLOBE* vector for knockdown of the γ-globin repressor *BCL11A.* Likewise expressing *HBB*$^{IVSI-110(G>A)}$-specific shRNA from *GLOBE* control elements or from within *GLOBE*-encoded *HBB* introns may therefore deserve investigation, as might selection of alternative promoters for earlier erythroid-lineage shRNA expression.

Applying our approach with treatment parameters suitable for clinical translation could significantly change gene therapy for patients with the *HBB*$^{IVSI-110(G>A)}$ or other mutations producing aberrant mRNAs. Besides higher vector yields and towards targeted gene addition for increased biosafety or exploitation of endogenous control elements,[22,23] the sequences required for shRNA-mediated knockdown provide shorter and more efficient integration templates than the large fragments required for *HBB* gene addition. Moreover, mutation-specific shRNAs alone or combined with gene addition may achieve transfusion independence at lower VCN or at milder conditioning regimens, thus improving biosafety and tolerability of therapy. We note that current trends in gene-therapy development for β-globinopathies favor editing (for potentially improved biosafety) or universal treatment approaches (for R&D profitability).[24] However, improvements in the efficiency of targeted gene addition have started to address biosafety for integrating vectors,[23] and changes in regulatory requirements, manufacturing cost and reimbursement policies may in the future favor more effective, stratified gene-therapy applications,[25] such as that proposed in this study. Our findings highlight the potential of shRNA-based therapies for other mutations and disorders associated with aberrant transcripts and stress the need to consider allelic heterogeneity in the application of gene therapy by gene addition.

Supplementary tables

Table S1. Primers and probes employed in this study

Name	Sequence 5' – 3'	Purpose
IVSI-110_Mut_FW IVSI-110_Mut_RV	CTC TCT CTG CCT ATT AGT CTA TTT TCC CAC CC GGG TGG GAA AAT AGA CTA ATA GGC AGA GAG AG	*HBB* mutagenesis *(Mutagenic nucleotide underlined)*
mHba FW mHba RV	GTCACGGCAAGAAGGTCGC GGGGTGAAATCGGCAGGGT	Measurement of total murine Hba mRNAs[26]
hHBB_FW_EX2_B hHBB_EX2.3_RV_B	GGC AAG AAA GTG CTC GG GTG CAG CTC ACT CAG TG	Measurement of total human *HBB* mRNA (exon 2)
HBB_Ex1_FW HBB_Ex2_RV A_MGB_VIC N_ZNA_FAM	GGG CAA GGT GAA CGT G GGA CAG ATC CCC AAA GGA C TAA GGG TGG GAA AAT AGA TGG G(PDC)A GG(PDC) TG(PDC) TG	Measurement of human *HBB* mRNA variants with common primers and aberrant-specific (A_MGB_VIC) and normal-specific (N_ZNA_FAM) probes

Table S2. Titers of lentiviral vectors employed in this study

Name	Final qPCR titer (TU/mL)
GLOBE	8.79×10^7
shRNA-Up	5.77×10^8
shRNA-Mid	3.92×10^8
shRNA-Mid2	2.30×10^8
shRNA-Down	7.76×10^8
shRNA-Scramble	2.30×10^9

Vector-containing supernatant was concentrated 350x and biologically titered in human erythroleukemia (HEL) cells by qPCR as described.[1] Exceptionally, GLOBE$^{IVSI\text{-}110(G>A)}$ was exclusively used for production of low-VCN transgenic MEL cells and was neither concentrated nor titered in HEL cells.

Supplementary figures and legends

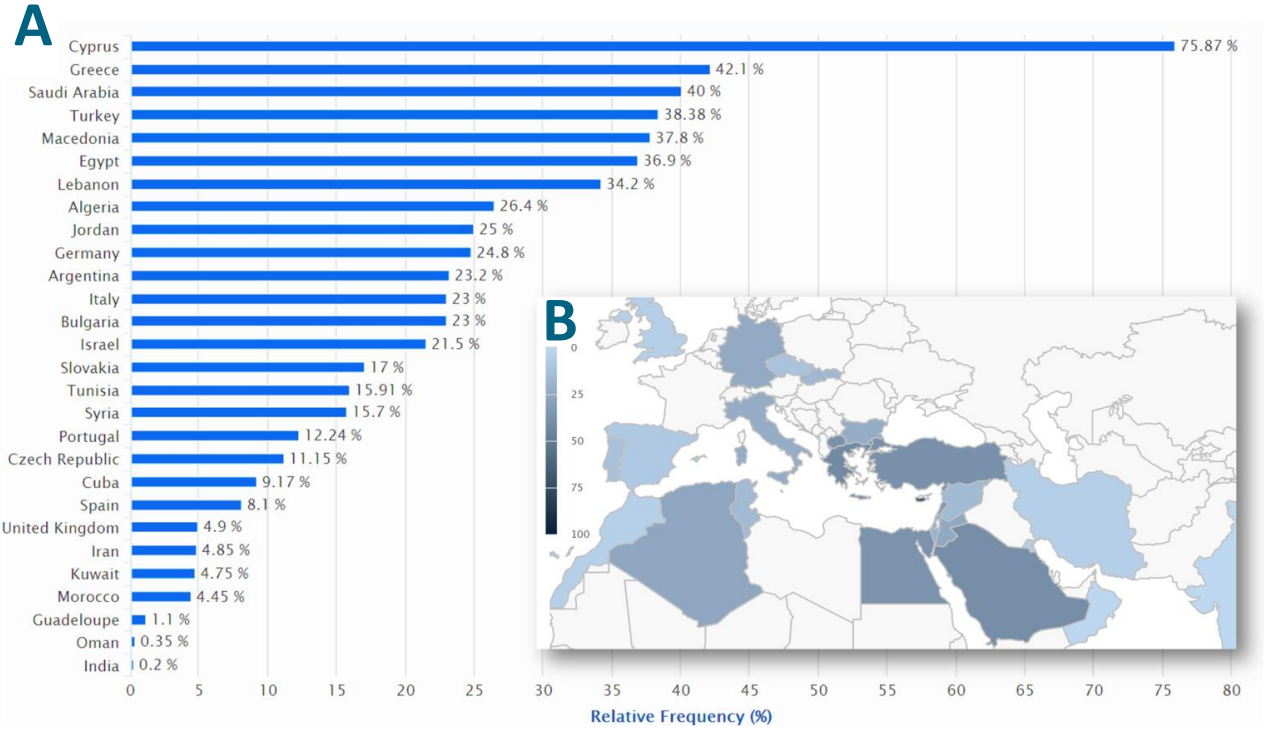

Supplementary Figure S1. Relative carrier frequencies of the* HBB$^{IVSI\text{-}110(G>A)}$ *mutation. A. Relative worldwide carrier frequencies of the *HBB*$^{IVSI\text{-}110(G>A)}$ mutation as reported in peer-reviewed publications or submitted directly to ITHANET, shown as countrywide averages. B. Corresponding view of national relative carrier frequencies (in %) with focus on Southern Europe and the Eastern Mediterranean. *Source: ITHANET (for (A) http://www.ithanet.eu/db/ithagenes?ithaID=113, for (B) http://www.ithanet.eu/db/ithamaps?ithaID=113); accessed 16 January 2018*

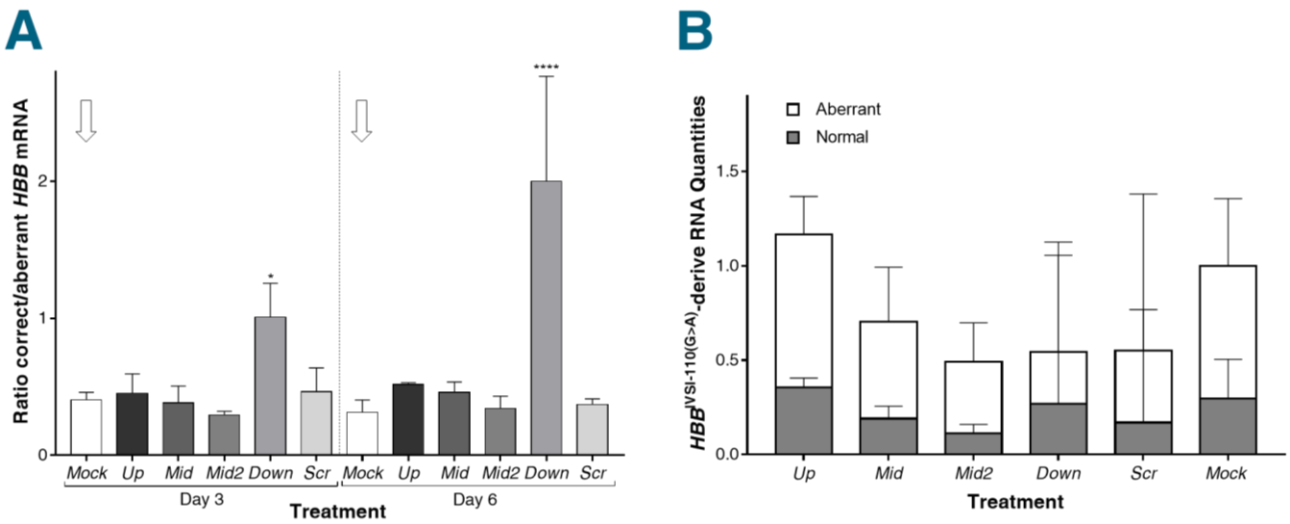

Supplementary Figure S2. RT-qPCR analysis of transduced MEL-*HBB^{IVS} *cells. A. Ratio of correct to aberrant mRNAs at days 3 and 6 of erythroid differentiation as determined by RT-qPCR (n=3). * – *P*=0.0136; **** – *P*<0.0001. B. Bar chart displaying the abundance of total *HBB* mRNA compared to *Mock* as stacked bar height and the contribution of aberrant and normal *HBB* transcripts as open and grey bar segments, respectively, for day 3 of erythroid differentiation. No significant differences were detected, in part owing to the great level of intra-group variation typical of heterogeneous erythroid cell populations and their substantial stage-specific differences in expression patterns.[26]

	Up	Mid	Mid2	Down	Scr	Mock	Up	Mid	Mid2	Down	Scr	Mock	Mock	Up	Mid	Mid2	Down	Scr	Mock	Mock
Actb	1463535	1763124	1798866	1896102	1547488	618936	1552278	1538495	1831880	1927600	2040880	2062920	1875040	1667316	1790460	2169510	2210250	1933344	1947876	1955352
HBB	1284704	12437058	12073018	2214146	1383618	3327964	1695681	10208835	11267080	4430840	2505360	1894720	2867520	664818	14589960	10681608	3501204	612906	836094	682584
Actb	1860180	2172059	1811676	1998296	1902836	900291	9943050	9218370	10451960	11363160	10602960	10841520	10036520	1975134	2055564	1873536	2007348	1810326	1737120	1706292
Hba	6465624	11520384	4631516	4669592	4888092	12358436	6052824	6993252	7143084	6639408	7351632	10078164	11624364	11923800	7781046	4582158	11215932	5711874	15527778	10588872
VCN	2.9	13.5	37.3	27.8	12.3	n/a	1.3	3.5	2.5	8.2	4.4	n/a	n/a	2.6	6.0	4.8	5.8	2.7	n/a	n/a

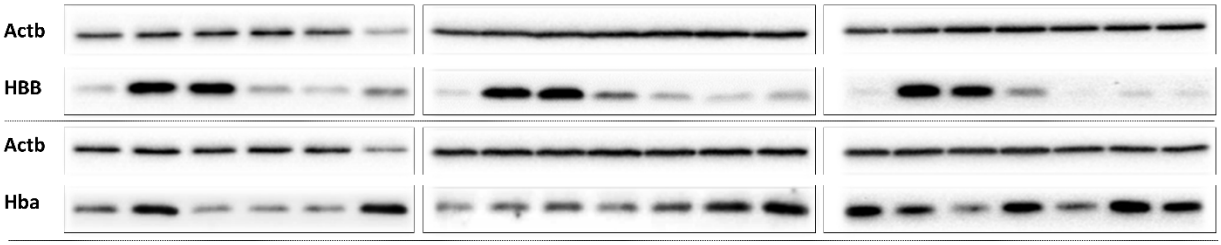

Supplementary Figure S3. Immunoblot analysis of transduced MEL-HBB^{IVS} cells with raw band intensities. The immunoblots shown in Figure 3C (n=3), including raw values of band intensities as measured for the unsaturated original images using ImageJ, and including VCN measurements for the three independent biological replicates. Despite differing VCNs, replicates gave comparable levels of HBB induction, indicating the robustness of the method. Of note, increased vector doses for *Up* in the MEL^{IVS} model led to disproportionate increase in cell death without concomitant increase in VCN.

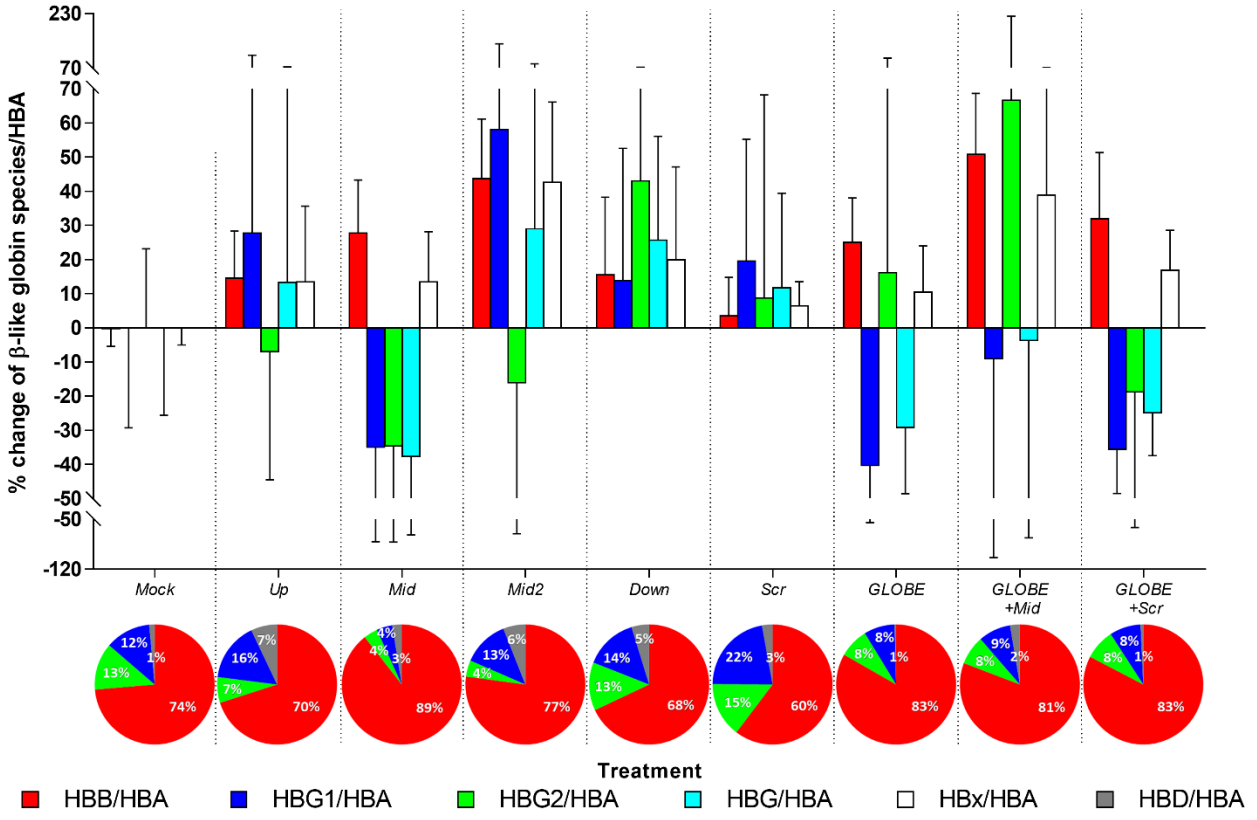

Supplementary Figure S4. Percentage change and average distribution of HBA-normalized β-like globins and combinations of interest. Bar charts show percentage changes for HBB/HBA, HBG1/HBA, HBG2/HBA, HBG/HBA and total β-like globin/HBA, as indicated using the rules for additive color mixing for bar colors, corresponding to same-sample HBB/HBA ratios compared to same-experiment *Mock* levels as detected by HPLC for Figure 3D. Variation across biological repeats based on different primary samples and at times detection close to baseline for γ-globin chains resulted in substantial variability in their detection. Pie charts show corresponding outlier-removed distributions of β-like globins across all experiments; this is only indicative of treatment effect and less representative than the average of same-experiment comparisons to *Mock* shown above. See Figure 3 for full sample details.

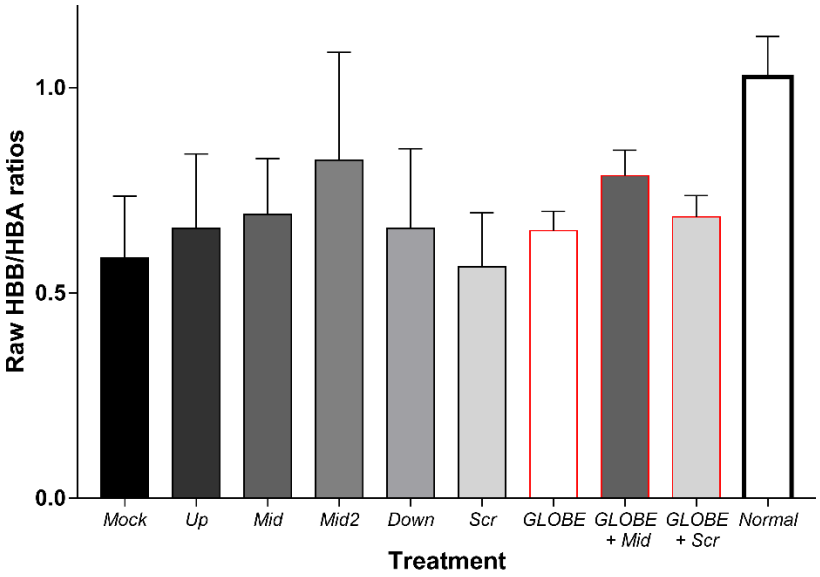

Supplementary Figure S5. Raw HBB/HBA ratios as measured by HPLC. Illustration of differentiation-corrected HBB expression for CD34⁺ cells from normal blood donors (n=2) and from thalassemic blood donors (see Figure 3 for full sample details) without additional normalization. The detected HBB/HBA ratios for different treatments do not take into account concurrent changes in insoluble, membrane-bound HBA.

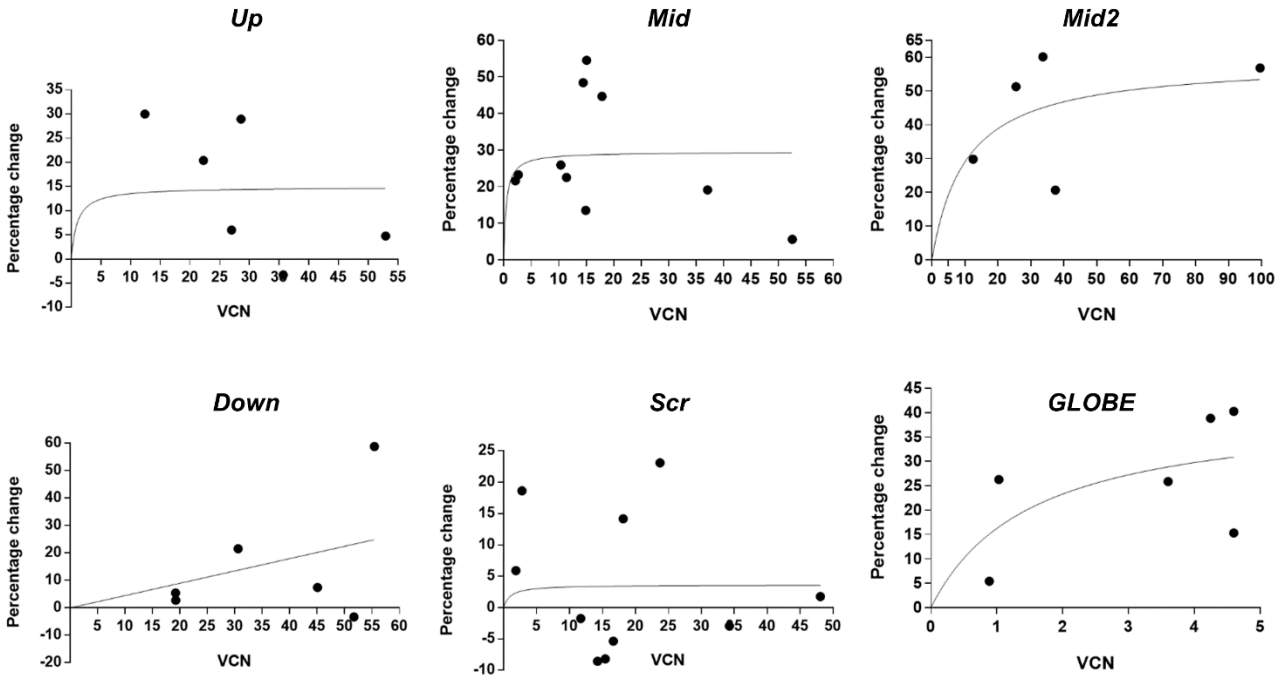

Supplementary Figure S6. Non-linear regression analysis. The percentage change of HBB/HBA compared to *Mock* in *HBB*$^{IVSI-110(G>A)}$-homozygous cells was blotted against the VCN determined by qPCR. All evaluable biological replicates for *Up* (n=6), *Mid* (n=10), *Mid2* (n=5), *Down* (n=6), *Scr* (n=10) and *GLOBE* (n=6) were included in the analysis without outlier removal, and curve fitting was constraint to a positive relationship of VCN and percentage change, and to include the origin (0/0) of the graph.

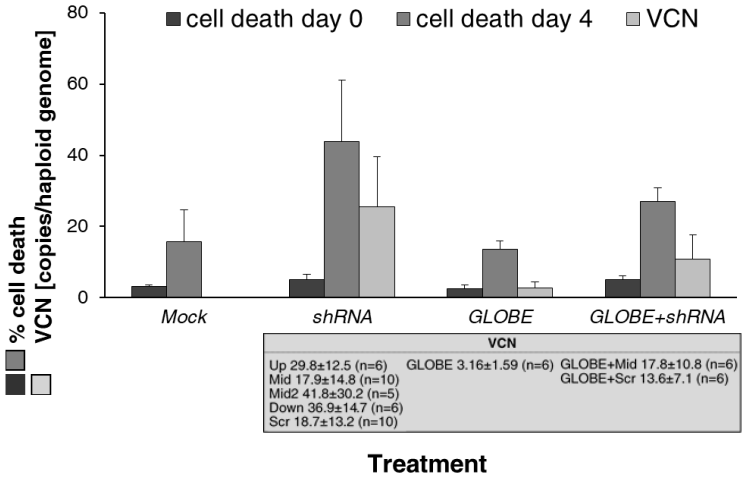

Supplementary Figure S7. Cell death and vector copy number by treatment category. Summarizing all transduction experiments in *HBB*$^{IVSI-110(G>A)}$-homozygous CD34^{+}-derived cultures, the bar chart shows cell death as a percentage of all cells three days after transduction at the start of differentiation (day 0, ■) and at the time of sample collection (day 4, ■), and the VCN as determined by qPCR (□). For combination treatments, VCN specifies the combined VCN of GLOBE and shRNA-encoding vectors. Samples are categorized into mock treatment, only (*Mock*), gene addition by the GLOBE LV, only (GLOBE), treatment with shRNA, only (shRNA) and combination treatment of GLOBE with either Scr or Mid shRNA (GLOBE+shRNA). Detailed VCN information for individual vectors and vector combinations is given below the category label.

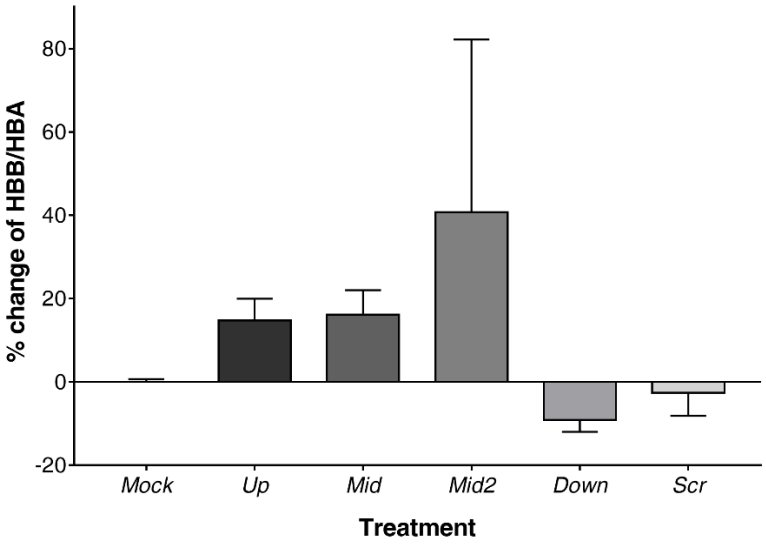

Supplementary Figure S8. Percentage change of HBB/HBA ratio in shRNA-treated normal CD34^{+} cells compared to Mock. CD34^{+} cells from normal blood donors were transduced with shRNA-encoding LVs and analyzed for changes in HBB/HBA ratio (n=2)

Supplementary references

1. Christodoulou I, Patsali P, Stephanou C, Antoniou M, Kleanthous M, Lederer CW. Measurement of lentiviral vector titre and copy number by cross-species duplex quantitative PCR. Gene Ther 2016;23(1):113–118.
2. Stephanou C, Papasavva P, Zachariou M, et al. Suitability of small diagnostic peripheral-blood samples for cell-therapy studies. Cytotherapy 2017;19(2):311–326.
3. Root DE, Hacohen N, Hahn WC, Lander ES, Sabatini DM. Genome-scale loss-of-function screening with a lentiviral RNAi library. Nat Methods 2006;3(9):715–719.
4. Miccio A, Cesari R, Lotti F, et al. In vivo selection of genetically modified erythroblastic progenitors leads to long-term correction of beta-thalassemia. Proc Natl Acad Sci U S A 2008;105(30):10547–10552.
5. Dessypris EN, Sawyer ST. Chapter 6: Erythropoiesis. In: Greer JP, editor. Wintrobe's Clinical Hematology, 12th Ed. Lippincott Williams & Wilkins; 2009.
6. Karponi G, Psatha N, Lederer CW, et al. Plerixafor+G-CSF-mobilized CD34+ cells represent an optimal graft source for thalassemia gene therapy. Blood 2015;126(5):616–619.
7. Nemati H, Bahrami G, Rahimi Z. Rapid separation of human globin chains in normal and thalassemia patients by RP-HPLC. Mol Biol Rep 2011;38(5):3213–3218.
8. Roselli EA, Mezzadra R, Frittoli MC, et al. Correction of beta-thalassemia major by gene transfer in haematopoietic progenitors of pediatric patients. EMBO Mol Med 2010;2(8):315–328.
9. Gu S, Jin L, Zhang F, et al. Thermodynamic stability of small hairpin RNAs highly influences the loading process of different mammalian Argonautes. Proc Natl Acad Sci U S A 2011;108(22):9208–9213.
10. Yordanova MM, Loughran G, Zhdanov A V., et al. AMD1 mRNA employs ribosome stalling as a mechanism for molecular memory formation. Nature 2018;553(7688):356–360.
11. Breda L, Casu C, Casula L, et al. Following Beta-Globin Gene Transfer, the Production of Hemoglobin Depends Upon the Beta-Thalassemia Genotype. Blood (ASH Annu Meet Abstr 2009;51st ASH A(114: Abstract 978):978–978.
12. Loucari CC, Patsali P, van Dijk TB, et al. Rapid and sensitive assessment of globin chains for gene and cell therapy of haemoglobinopathies. Hum Gene Ther Methods 2018;29(1):hgtb.2017.190 (15 pages).
13. Lee NS, Kim DH, Alluin J, et al. Functional and intracellular localization properties of U6 promoter-expressed siRNAs, shRNAs, and chimeric VA1 shRNAs in mammalian cells. RNA 2008;14(9):1823–33.
14. Langlois M-A, Boniface C, Wang G, et al. Cytoplasmic and Nuclear Retained DMPK mRNAs Are Targets for RNA Interference in Myotonic Dystrophy Cells. J Biol Chem 2005;280(17):16949–16954.
15. El-Beshlawy A, Mostafa A, Youssry I, et al. Correction of aberrant pre-mRNA splicing by antisense oligonucleotides in beta-thalassemia Egyptian patients with IVSI-110 mutation. J Pediatr Hematol Oncol 2008;30(4):281–284.
16. Imbert M, Dias-Florencio G, Goyenvalle A. Viral Vector-Mediated Antisense Therapy for Genetic Diseases. Genes (Basel) 2017;8(2):51 (19 pages).
17. Godfrey C, Desviat LR, Smedsrød B, et al. Delivery is key: lessons learnt from developing splice-switching antisense therapies. EMBO Mol Med 2017;9(5):545–557.
18. Manjunath N, Wu H, Subramanya S, Shankar P. Lentiviral delivery of short hairpin RNAs. Adv Drug Deliv Rev 2009;61(9):732–745.
19. Lin S-L, Miller JD, Ying S-Y. Intronic microRNA (miRNA). J Biomed Biotechnol 2006;2006(4):26818 (13 pages).
20. Samakoglu S, Lisowski L, Budak-Alpdogan T, et al. A genetic strategy to treat sickle cell anemia by coregulating globin transgene expression and RNA interference. Nat Biotechnol 2006;24(1):89–94.
21. Brendel C, Guda S, Renella R, et al. Lineage-specific BCL11A knockdown circumvents toxicities and reverses sickle phenotype. J Clin Invest 2016;126(10):3868–3878.
22. Lombardo A, Cesana D, Genovese P, et al. Site-specific integration and tailoring of cassette design for sustainable gene transfer. Nat Methods 2011;8(10):861–869.
23. Genovese P, Schiroli G, Escobar G, et al. Targeted genome editing in human repopulating haematopoietic stem cells. Nature 2014;510(7504):235–240.
24. Lederer CW, Kleanthous M. Beta testing : preclinical genome editing in β-globin disorders. Cell Gen Ther Insights 2015;1(2):231–242.
25. Mount NM, Ward SJ, Kefalas P, Hyllner J. Cell-based therapy technology classifications and translational challenges. Philos Trans R Soc Lond B Biol Sci 2015;370(1680):20150017 (16 pages).
26. Cells RED, An X, Schulz VP, et al. Global transcriptome analyses of human and murine terminal erythroid differentiation. Blood 2014;123(22):3466–3477.